



Evolution of fusion hindrance for asymmetric systems at deep sub-barrier energies

A. Shrivastava^{a,b,*}, K. Mahata^{a,b}, S.K. Pandit^{a,b}, V. Nanal^c, T. Ichikawa^d, K. Hagino^e,
A. Navin^f, C.S. Palshetkar^a, V.V. Parkar^a, K. Ramachandran^{a,b}, P.C. Rout^{a,b},
Abhinav Kumar^a, A. Chatterjee^a, S. Kailas^a

^a Nuclear Physics Division, Bhabha Atomic Research Centre, Mumbai 400085, India

^b Homi Bhabha National Institute, Anushaktinagar, Mumbai 400094, India

^c DNAP, Tata Institute of Fundamental Research, Mumbai 400005, India

^d Yukawa Institute for Theoretical Physics, Kyoto University, Kyoto 606-8502, Japan

^e Department of Physics, Tohoku University, Sendai 980-8578, Japan

^f GANIL, CEA/DRF – CNRS/IN2P3, Bd Henri Becquerel, BP 55027, F-14076 Caen Cedex 5, France

ARTICLE INFO

Article history:

Received 2 October 2015

Received in revised form 28 January 2016

Accepted 15 February 2016

Available online 19 February 2016

Editor: V. Metag

Keywords:

Fusion cross sections

Deep sub-barrier energies

Coupled channels calculations

Adiabatic model

ABSTRACT

Measurements of fusion cross-sections of ${}^7\text{Li}$ and ${}^{12}\text{C}$ with ${}^{198}\text{Pt}$ at deep sub-barrier energies are reported to unravel the role of the entrance channel in the occurrence of fusion hindrance. The onset of fusion hindrance has been clearly observed in ${}^{12}\text{C} + {}^{198}\text{Pt}$ system but not in ${}^7\text{Li} + {}^{198}\text{Pt}$ system, within the measured energy range. Emergence of the hindrance, moving from lighter (${}^{6,7}\text{Li}$) to heavier (${}^{12}\text{C}$, ${}^{16}\text{O}$) projectiles is explained employing a model that considers a gradual transition from a sudden to adiabatic regime at low energies. The model calculation reveals a weak effect of the damping of coupling to collective motion for the present systems as compared to that obtained for systems with heavier projectiles.

© 2016 The Authors. Published by Elsevier B.V. This is an open access article under the CC BY license (<http://creativecommons.org/licenses/by/4.0/>). Funded by SCOAP³.

1. Introduction

Fusion reactions in the vicinity of the Coulomb barrier have been investigated in the past to explore the mechanism of tunneling through multidimensional barriers, thereby giving an insight into the role of different intrinsic properties of the entrance channel. Recent efforts towards developing new methods to precisely measure very low fusion cross-sections have stimulated new activities, distinct to energies deep below the barrier. Fusion data at these low energies can be uniquely used to interpret the reaction dynamics from the touching point to the region of complete overlap of the density distribution of the colliding nuclei, not accessible through any other reaction [1,2]. This opens up the possibility to study effects of dissipative quantum tunneling, which has relevance in many fields of physics and chemistry [3]. The data in this energy range was shown to have strong implications on the fusion with light nuclei of astrophysical interest [2].

At deep sub-barrier energies, a change of slope of the fusion excitation function compared to coupled-channels (CC) calculations

was observed initially in symmetric systems involving medium-heavy nuclei and was referred to as the phenomenon of fusion hindrance [4,5]. The models suggested to explain this behavior have different physical basis. The model proposed by Mişicu and Esbensen is based on a sudden approximation [6], where a repulsive core is included to take into account the nuclear compressibility arising due to Pauli exclusion principle when the two nuclei overlap. On the other hand at low energies, the nucleus–nucleus interaction potentials extracted from the microscopic time-dependent Hartree–Fock theory indicate that after overlap of two nuclei, internal degrees of freedom reorganize adiabatically [7]. The model proposed by Ichikawa et al. [8] to explain the deep sub-barrier fusion data is based on such an adiabatic picture. Here a damping factor imposed on the coupling strength as a function of the inter-nuclear distance, takes into account a gradual change from the sudden to the adiabatic formalism [9,10]. A recent work, applying the random-phase-approximation (RPA) demonstrates that the fusion hindrance originates from damping of quantum vibrations when the two nuclei adiabatically approach each other [11, 12]. The role of quantum de-coherence that effectively causes a reduction in coupling effects has also been investigated [13,14].

* Corresponding author.

E-mail address: aradhana@barc.gov.in (A. Shrivastava).

In all the above models, fusion hindrance is a generic property of heavy-ion collision below certain threshold energy. Due to challenges involved with measurement of low cross-section (\sim nb), there are only a limited number of studies involving fusion hindrance. As discussed in a recent review article [2], these studies have mainly concentrated around medium-heavy ($A \sim 100$), medium ($A \sim 50$) and light ($A \sim 10$) symmetric systems [4,5,15–21], covering a wide range of reduced masses, Q-values and nuclear structure properties. Most of the measurements employed recoil mass analyzers and hence are restricted to symmetric or nearly symmetric systems. In such cases the evaporation residues have sufficient recoil velocities for being detected at the focal plane of the spectrometer. The data corresponding to asymmetric systems, presently scarce, are vital to establish the generic nature of the fusion hindrance and for the improvement of current theoretical models. The only exception being the two systems $^{16}\text{O} + ^{208}\text{Pb}$ [14] and $^6\text{Li} + ^{198}\text{Pt}$ [22] that used different methods for fusion cross-section measurements. The presence of fusion hindrance was clearly shown in $^{16}\text{O} + ^{208}\text{Pb}$ system [14]. The shapes of the logarithmic derivative and astrophysical S-factor for this asymmetric system were found to be different, compared to those for the symmetric systems [1,2]. In the case of a more asymmetric system $^6\text{Li} + ^{198}\text{Pt}$ [22], an absence of fusion hindrance was reported at energies well below the threshold energy (E_T) computed from both the sudden and adiabatic models. For reactions induced by protons, intuitively one would not expect fusion hindrance. In this case, the projectile maintains its identity and the sudden approximation would be appropriate. This should be the case for alpha particle as well, which can be treated as a rigid nucleus. On the other hand for heavier projectiles, such as ^{12}C and ^{16}O , one may expect a neck formation at low energies when the colliding nuclei follow the minimum energy path allowing for the readjustment of the densities as a function of the collective variables. Deviation from a simple sudden picture is expected to occur for nuclei heavier than ^4He .

The present work investigates the evolution of the fusion hindrance with increasing mass and charge of relatively light projectiles (^6Li , ^{12}C , ^{16}O) on heavy targets. For this purpose we have performed new measurements at deep sub-barrier energies with ^7Li and ^{12}C projectiles on a ^{198}Pt target. The current results along with the available data for different entrance channels have been studied to understand the origin of the fusion hindrance.

2. Experimental details and results

The experiments were performed at the Pelletron-Linac Facility, Mumbai, using beams of ^7Li (20–35 MeV) and ^{12}C (50–64 MeV) on a ^{198}Pt target with beam current in the range of 10 to 35 pA. The targets were foils of ^{198}Pt (95.7% enriched, ~ 1.3 mg/cm 2 thick) followed by an Al catcher foil of thickness ~ 1 mg/cm 2 . The cross-sections have been extracted using a sensitive and selective offline method employing KX- γ ray coincidence [22,23]. Two efficiency calibrated HPGe detectors – one with an Al window for detection of γ -rays and another with a Be window for detection of KX-rays, having an active volume ~ 180 cc were placed face to face for performing KX- γ -ray coincidence of the decay radiations from the irradiated sample. The irradiated targets were mounted at ~ 1.5 mm from the face of each detector. The measurements were performed in a low background setup with a graded shielding (Cu, Cd sheets of thickness ~ 2 mm followed by 10 cm Pb). The evaporation residues from complete fusion were uniquely identified by means of their characteristic γ -ray energies and half-lives which correspond to $^{205-207}\text{Po}$ in case of $^{12}\text{C} + ^{198}\text{Pt}$ and $^{200-202}\text{Tl}$ in case of $^7\text{Li} + ^{198}\text{Pt}$ systems. The γ -ray yields of the daughter nuclei at lowest energies were extracted by gating on their KX-ray transi-

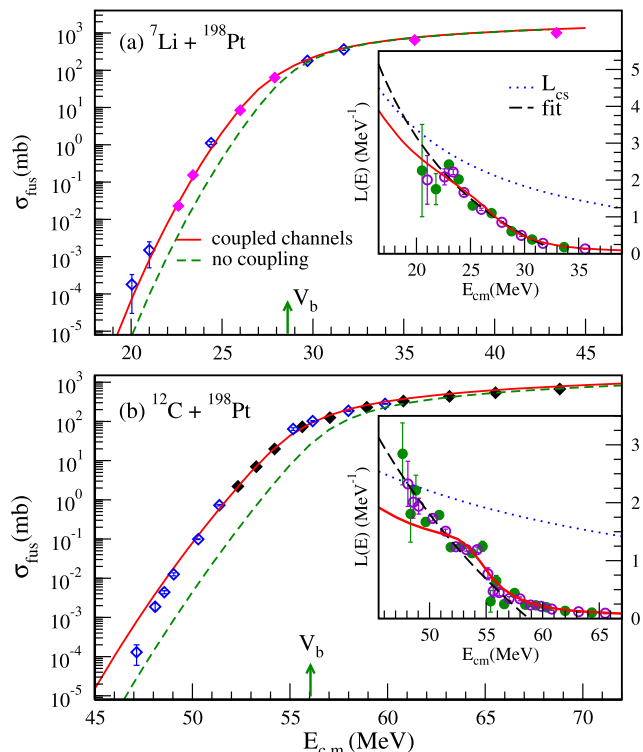


Fig. 1. (Color online.) Fusion excitation function and its logarithmic derivative (inset) for (a) $^7\text{Li} + ^{198}\text{Pt}$ and (b) $^{12}\text{C} + ^{198}\text{Pt}$ systems. The arrow indicates the value of the Coulomb barrier (V_b). The cross-sections from Refs. [25,27] are shown as filled diamonds. The $L(E)$ values shown as closed and open circles were obtained from two consecutive data points and least-squares fits to three successive data points, respectively. The results of the coupled-channels calculations (solid line) along with single channel calculations (dashed line) using the code CCFULL are also shown. The $L(E)$ values fitted to an expression and that corresponding to a constant S-factor ($L_{\text{cs}}(E)$) are shown as long dashed and dotted curves, respectively (see text).

tions. Further details on the method can be found in Ref. [23]. Due to the increased sensitivity of the KX- γ -ray coincidence method, cross-section down to 130 nano-barns could be measured. The fusion cross-sections were obtained from the sum of the measured evaporation residue cross-sections. In case of $^{12}\text{C} + ^{198}\text{Pt}$ system, the fission cross-section was also taken into account using data from Ref. [25], up to the beam energy where fission cross-section was $\sim 0.5\%$ of the fusion cross-section. The statistical model calculations for the compound nuclear decay were performed using PACE [24] with parameters from Refs. [22,25] which reproduce the residue cross-sections well for both the systems. The estimation of errors for low counting rates was made assuming Poisson statistics and using the method of maximum likelihood [26]. The present results are shown in Fig. 1, together with the cross-sections obtained in Refs. [25,27]. The error on the data points in Fig. 1 is only statistical in nature.

Plotted in the inset of Fig. 1(a) and (b) are the logarithmic derivatives of the fusion cross-section ($L(E) = d[\ln(\sigma_{\text{fus}})]/dE$), determined using two consecutive data points and also performing a least square fit to a set of three data points. This representation provides an alternate way to illustrate any deviations in the slope of the fusion excitation function independent of the weight of the lowest barrier [2]. The $L(E)$ values fitted to the expression ($A + B/E^{3/2}$) and that corresponding to a constant astrophysical S-factor ($L_{\text{cs}}(E)$) [28] are shown as long dashed and dotted lines respectively. The cross-over point between the $L(E)$ and $L_{\text{cs}}(E)$ corresponds to peak of the S-factor and can be related to the threshold energy for observing fusion hindrance [28].

3. Calculations

Coupled-channels calculations using the code CCFULL [29] were performed for both the systems. In the case of ${}^7\text{Li} + {}^{198}\text{Pt}$ system, a standard Woods–Saxon potential (WS) was used with $V_0 = 110$ MeV, $r_0 = 1.1$ fm and $a = 0.63$ fm. These calculations included two phonon quadrupole excitation of ${}^{198}\text{Pt}$ in the vibrational and the first excited state of ${}^7\text{Li}$ in the rotational mode. The CC calculations reproduce the data well for energies around and well below the barrier as seen in Fig. 1(a). Fusion hindrance has not been observed in this system in the measured energy range with the cross-section as low as ≈ 180 nb. The threshold energy for observing fusion hindrance obtained from the systematics of Ref. [30] and the adiabatic model [8] is 20.4 MeV and 21.1 MeV, respectively. However, from an extrapolation of the experimental data, this energy is found to be ≈ 19 MeV (Fig. 1(a) inset). Hence it will be interesting to extend the measurement of fusion cross-sections below the lowest energy of the present measurement (20 MeV).

The corresponding calculations for ${}^{12}\text{C} + {}^{198}\text{Pt}$ were performed using a WS potential with $V_0 = 95$ MeV, $r_0 = 1.13$ fm and $a = 0.66$ fm. The coupling to the quadrupole phonon excitation for ${}^{198}\text{Pt}$ and the first two excited states of ${}^{12}\text{C}$ belonging to the ground state rotational band were included. The quadrupole and hexadecapole deformation parameters used were taken from Ref. [31]. The effect of coupling to the ${}^{12}\text{C}$ rotational states is not as strong as in the well deformed heavy nuclei. Coupling to one neutron, two neutron and one proton transfer reaction were not included in the present scheme as their effect was found to be negligible for this system [25]. The result from the CC calculations are compared with the experimental data in Fig. 1(b). A change of slope as compared to CC calculations is clearly observed, both in the measured fusion excitation function as well as in the $L(E)$ plot, confirming the onset of fusion hindrance. The energy at which the deviation in the slope occurs was estimated to be 50 ± 1 MeV using the method described in Ref. [32]. The calculated threshold energy according to the adiabatic model [8] is 49 MeV while that from the systematics (43.7 MeV) [30] is much lower than the observed value.

In order to explain the fusion data at energies deep below the barrier in case of ${}^{12}\text{C} + {}^{198}\text{Pt}$ system, calculations were performed using the adiabatic model of Refs. [9,10]. This model employs a gradual diminishing of the coupling strength while going from the two body sudden to one body adiabatic potential as the two nuclei begin to overlap. The calculations adopted a Yukawa-plus-exponential (YPE) potential as a basic ion–ion potential with radius, $r_0 = 1.20$ fm and diffuseness, $a = 0.68$ fm. The coupling scheme was the same as that described earlier for this system. The calculated fusion cross-sections without damping, shown as the dot-dashed curves in Fig. 2(a), already provide a good fit, although the calculation underestimates the data for $L(E)$ at the lowest energies (see Fig. 2(b)). The calculations shown here differ slightly from those in Fig. 1(b). This is due to the use of different potentials (YPE and Woods–Saxon) in these two calculations, and the fact that the YPE potential is thicker than the Woods–Saxon potential (due to the saturation condition at the touching point in the YPE potential). Further discussion about the choice of potentials used in the present work can be found in section IIC of Ref. [10]. Fig. 2 also shows the results of the calculation with the inclusion of a damping factor ($r_{damp} = 1.18$ fm and $a_{damp} = 0.5$ fm), which are in excellent agreement with both the fusion and the $L(E)$ data. As can be seen from the figure, the effect of the damping is observed to be small in the present case when compared to that observed in studies involving heavier projectiles [10]. A systematic investigation of various systems showed that the radius parameter, related to the density distribution of the colliding nuclei, is almost con-

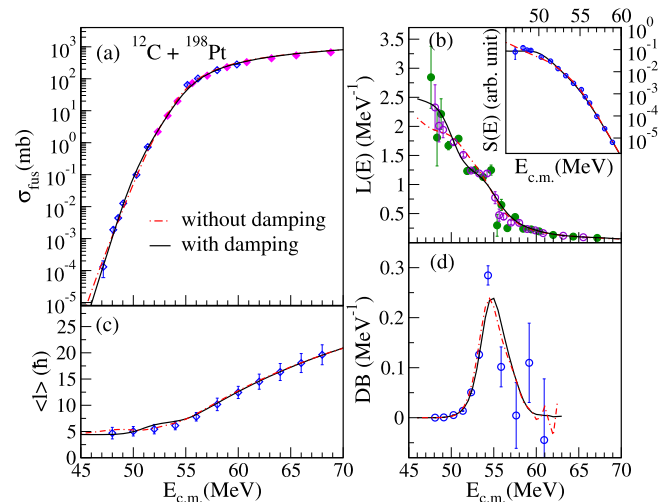


Fig. 2. (Color online.) Results from the adiabatic model calculation for ${}^{12}\text{C} + {}^{198}\text{Pt}$ system compared with the experimental (a) fusion cross-sections, (b) logarithmic derivative along with S-factor (inset), (c) average angular momentum and (d) fusion barrier distribution. Calculations using with and without a damping factor for the coupling strength are shown as solid and dashed-dot curves respectively.

stant [10]. On the other hand a_{damp} , associated with the damping strength of quantum vibrations that depends on the structure of interacting nuclei, was found to vary between 0.5 and 1.2 fm. The values of r_{damp} and a_{damp} obtained in the present work are within the range of the values reported in Ref. [10].

The adiabatic calculations were compared with other observables derived from the fusion data. The astrophysical S-factor representation ($S(E)$) of the experimental data is shown in the inset of Fig. 2(b). The observed S-factor maximum is not as pronounced as found for the case of the symmetric systems involving medium mass nuclei, but similar to that for ${}^{16}\text{O} + {}^{208}\text{Pb}$ system [1,2,33]. The calculated $S(E)$ match well with the data over the entire energy range. The average angular momenta ($\langle l \rangle$) computed from the fusion excitation function as suggested in Ref. [34] and the fusion barrier distribution (DB) are also well described by the adiabatic calculation (Fig. 2(c) and (d)).

Similar calculations were performed for ${}^7\text{Li} + {}^{198}\text{Pt}$ using the YPE potential ($r_0 = 1.195$ fm and $a = 0.68$ fm) with the coupling scheme being the same as that described above for this system. The calculations explain the data well up to the measured energy. The values of r_{damp} and a_{damp} can not be determined uniquely with the present data as no change of slope of the fusion excitation function was observed. For example, values of the damping factor parameters $r_{damp} = 1.16$ fm and $a_{damp} = 0.5$ fm, would give rise to a small deviation in the slope at energy ~ 19 MeV. The threshold energy for observing hindrance is expected to be below this value.

4. Discussion

We now discuss the general trend of fusion excitation function at deep sub-barrier energies for asymmetric systems involving light projectiles, namely, ${}^6\text{Li} + {}^{198}\text{Pt}$ [22], ${}^7\text{Li} + {}^{198}\text{Pt}$, ${}^{12}\text{C} + {}^{198}\text{Pt}$ and ${}^{16}\text{O} + {}^{208}\text{Pb}$ [14,35]. ${}^6,7\text{Li} + {}^{198}\text{Pt}$ are among the few systems, that have been probed for hindrance studies, having positive Q-values for the formation of compound nucleus [2]. As ${}^6,7\text{Li}$ are weakly bound nuclei (${}^6\text{Li}$, $S_{\alpha/d} = 1.47$ MeV and ${}^7\text{Li}$, $S_{\alpha/t} = 2.47$ MeV), the role of the breakup channel at energies relevant to the fusion hindrance needs to be considered as well. The influence of breakup on fusion and total reaction cross-sections has been extensively investigated [36,37]. Recent studies have also illustrated the importance of transfer followed by breakup channels [38,39].

- [4] C.L. Jiang, et al., Phys. Rev. Lett. 89 (2002) 052701.
- [5] C.L. Jiang, et al., Phys. Rev. Lett. 93 (2004) 012701.
- [6] S. Mišiću, H. Esbensen, Phys. Rev. Lett. 96 (2006) 112701;
S. Mišiću, H. Esbensen, Phys. Rev. C 75 (2007) 034606.
- [7] K. Washiyama, D. Lacroix, Phys. Rev. C 78 (2008) 024610;
A.S. Umar, V.E. Oberacker, Phys. Rev. C 74 (2006) 021601(R).
- [8] T. Ichikawa, K. Hagino, A. Iwamoto, Phys. Rev. C 75 (2007) 057603;
T. Ichikawa, K. Hagino, A. Iwamoto, Phys. Rev. C 75 (2007) 064612.
- [9] T. Ichikawa, K. Hagino, A. Iwamoto, Phys. Rev. Lett. 103 (2009) 202701;
T. Ichikawa, K. Hagino, A. Iwamoto, Prog. Theor. Phys. Suppl. 196 (2012) 269.
- [10] Takatoshi Ichikawa, Phys. Rev. C 92 (2015) 064604.
- [11] Takatoshi Ichikawa, Kenichi Matsuyanagi, Phys. Rev. C 88 (2013) 011602(R).
- [12] Takatoshi Ichikawa, Kenichi Matsuyanagi, Phys. Rev. C 92 (2015) 021602(R).
- [13] A. Diaz-Torres, et al., Phys. Rev. C 78 (2008) 064604;
A. Diaz-Torres, et al., Phys. Rev. C 81 (2010) 041603(R).
- [14] M. Dasgupta, et al., Phys. Rev. Lett. 99 (2007) 192701.
- [15] C.L. Jiang, et al., Phys. Rev. C 71 (2005) 044613.
- [16] A.M. Stefanini, et al., Phys. Rev. C 82 (2010) 014614.
- [17] C.L. Jiang, et al., Phys. Rev. C 82 (2010) 041601.
- [18] G. Montagnoli, et al., Phys. Rev. C 85 (2012) 024607;
G. Montagnoli, et al., Phys. Rev. C 82 (2010) 064609.
- [19] G. Montagnoli, et al., Phys. Rev. C 87 (2013) 014611.
- [20] A.M. Stefanini, et al., Phys. Lett. B 728 (2014) 639.
- [21] C.L. Jiang, et al., Phys. Rev. Lett. 113 (2014) 022701.
- [22] A. Shrivastava, et al., Phys. Rev. Lett. 103 (2009) 232702.
- [23] A. Lemasson, et al., Nucl. Instrum. Methods A 598 (2009) 445.
- [24] A. Gavron, Phys. Rev. C 21 (1980) 230.
- [25] A. Shrivastava, et al., Phys. Rev. Lett. 82 (1999) 699;
A. Shrivastava, et al., Phys. Rev. C 63 (2001) 054602.
- [26] W.-M. Yao, et al., J. Phys. G 33 (2006) 1.
- [27] A. Shrivastava, et al., Phys. Lett. B 718 (2013) 931.
- [28] C.L. Jiang, et al., Phys. Rev. C 73 (2006) 014613.
- [29] K. Hagino, et al., Comput. Phys. Commun. 123 (1999) 143.
- [30] C.L. Jiang, et al., Phys. Rev. C 79 (2009) 044601.
- [31] M. Yasue, et al., Nucl. Phys. A 394 (1983) 29.
- [32] Ei Shwe Zin Thein, N.W. Lwin, K. Hagino, Phys. Rev. C 85 (2012) 057602.
- [33] C.L. Jiang, et al., Phys. Rev. C 75 (2007) 057604.
- [34] A.B. Balantekin, P.E. Reimer, Phys. Rev. C 33 (1986) 379;
C.V.K. Baba, Nucl. Phys. A 553 (1993) 719c.
- [35] C.R. Morton, et al., Phys. Rev. C 60 (1999) 044608.
- [36] L.F. Canto, P.R.S. Gomes, R. Donangelo, J. Lubian, M.S. Hussein, Phys. Rep. 596 (2015) 1.
- [37] X.P. Yang, G.L. Zhang, H.Q. Zhang, et al., Phys. Rev. C 87 (2013) 014603.
- [38] D.H. Luong, et al., Phys. Lett. B 695 (2011) 105.
- [39] A. Shrivastava, et al., Phys. Lett. B 633 (2006) 433.
- [40] C.L. Jiang, et al., Phys. Rev. C 75 (2007) 015803.
- [41] L.R. Gasques, et al., Phys. Rev. C 76 (2007) 035802.